Response to Anonymous Referee #1

We would like to thank Referee #1 for the thorough review and constructive comments. We have carefully considered and addressed all comments, and significantly revised our manuscript. Please find our point-by-point response below. For clarity, the reviewer's comments are listed in black, while our response are shown in blue.

"A nicely written manuscript about downscaling of global reanalyses for regional climate modeling studies. I have no major comments, there are some spelling mistakes and incomplete sentences, but I am sure they will get corrected during the editing process."

Author Response: We would like to thank the reviewer for your positive comments on our study. We have taken each comment into account and revised our manuscript accordingly.

"I was missing a slightly more in-depth dynamical interpretation of why the best performing set of parameters improved the skill of WRF as an RCM."

Author Response: Thank you for this comment. To address this question, it is necessary to clarify the systematic inability of regional climate models first. Generally, a full forecast model within the regional domain can be decomposed into two components: the base field and the perturbation field. The base field is obtained from the driving fields, while the regional perturbation field is defined as the difference between the total field and the base field (Juang and Kanamitsu, 1994). Because of the systematic error of RCM, the inconsistencies between the model solution and the driving fields along the boundaries can cause large-scale errors (e.g., erroneous long waves), which might develop within the regional domain and produce undesirable noise.

In this case, spectral nudging technique is used to incorporate the large internal scales from outer model into the regional domain by adding a nudging term to the tendencies of nudged variables in model fields (Waldron et al., 1996). The nudging term is the summation of the difference between the spectrally expanded base field and the model field, multiplied by the nudging coefficients over selected wavenumbers. By applying spectral nudging technique, perturbation tendencies (a difference between the computed full field tendencies and the base field tendencies) are transformed to spectral space in RCM. Then, the spectral truncation filters out those waves longer than the regional domain from the perturbation tendencies. As a result, any scales longer than the regional domain cannot be modified during the course of integration (Kanamaru and Kanamitsu, 2007). Therefore, the large-scale information is retained and small-scale information can be freely resolved in downscaling process.

From the dynamical perspective, the best performing set of parameters of spectral nudging in this study is a combination of three corrections. For horizontal winds, spectral nudging determines the tendency of wind field perturbation whose scale was larger than the wavelength of 1000 km, so that the inconsistencies between the regional field and the base field can be alleviated. Nudging to geopotential height corrects the erroneous pressure difference due to the surface elevation difference between the ERA-Interim and WRF

model, leading to a better resolved topography of the Himalayas in the inner domain. For the temperature and humidity, their nudging coefficients were set to zero, which means their mean perturbations were set to zero, preventing the external forces on moisture and temperature (from nudging) to affect small-scale dynamics. In summary, nudging to winds and geopotential is strong enough to reduce large-scale errors in the regional domain, and this method improves the skill of WRF as a RCM.
Aforementioned dynamic interpretations of how spectral nudging influences the solution of RCM and how the set of spectral nudging parameters improved the skill of WRF have been added in 'Section 2.2' (Line 126-130) and 'Section 4.3' (Line 331-338) in the revised manuscript, respectively.

"Line 117-118: (incomplete sentence) Why did you use Yonsei scheme? I am assuming it is for the PBL."

Author Response: Thank you for this comment. A misleading sentence exists in the original manuscript. Actually, most physical options used in this study are the same as the options of the High Asia Refined (HAR) data. But for PBL scheme, we selected the YSU PBL scheme rather than Eta similarity PBL scheme. In the revised manuscript, relevant content has been revised as follows.
Line 118-119: 'The Yonsei University scheme (Hong et al., 2006) was used for the PBL scheme.'

"Line 145: Is the 'ktrop' option for spectral nudging now available to the larger audience of WRF users?"

Author Response: Thank you for this comment. To our knowledge, this new 'ktrop' option has been added in the released WRF model v4.0, and WRF users can use this option via 'namelist.input'. More details and usages about 'ktrop' are available from the source code 'WRF/phys/module_fdda_spnudging.F' (https://github.com/wrf-model/WRF/blob/master/phys/module_fdda_spnudging.F#L266).

"Line 276: 'transporting emissions - which emissions?"

Author Response: Thank you for this comment. The 'emissions' here means water vapor. In the revised manuscript, relevant text now reads:
Line 304-307: 'Deep convection favors the process of transporting water vapor into the upper-level atmosphere, through which moisture flux is vertically released into the atmosphere and influences the formation of precipitation during summer monsoon season (Fu et al., 2006; Heath and Fuelberg, 2014).'

"Line 285: By 'drag force', do you mean orographic blocking? What is the convergence of the water vapor? Please clarify."

Author Response: Yes, 'drag force' here is relevant to the orographic blocking. Specifically, it means the sub-grid orographic drag on water vapor due to the complex terrain over the southern slope of the Himalayas.

The convergence of water vapor is mainly caused by the barrier effect of the Himalayas, which are more than 5,000 m on average. In summer, abundant northward water vapor transport, originating from the surrounding oceans, impinges on the Himalayas. Upslope moisture transport is strictly limited by the sufficiently high orograph, and thus most of water vapor are 'wrung out' here, causing the convergence of water vapor (Dong et al., 2016).

To our knowledge, model with coarse spatial resolution ignores the impact of mesoscale and microscale orography. Accordingly, the surface friction and turbulent form drag on airflow with water vapor are reduced (Wang et al., 2020). Therefore, the convergence and condensation of water vapor over the southern slope of the Himalayas are weakened. In this case, more water vapor can be transported to the higher area and even the interior of the Tibetan Plateau.

Relevant text has been added to the revised manuscript as follows:

Line 268-277: 'The terrain of the Himalayas, featured by a sharp topography gradient, is more than 5,000 m on average and is regarded as a natural barrier for northward atmospheric flow. In summer, large amount of atmospheric water vapor transport, originating from the surrounding oceans, impinges on the Himalayas. The sufficient high topography strictly limits the upslope water vapor transport, and strong upward motions are consequently formed by the lifting effect of the complex terrain (Dong et al., 2016). However, the complex orography of the southern slope of the Himalayas is greatly smoothed in current RCMs. Accordingly, the surface friction and sub-grid orographic drag due to the impact of mesoscale and microscale orography on the airflow are weakened, which in turn reduce the convergence and condensation of water vapor over the southern slope of the Himalayas. Consequently, more water vapor transport could arrive the high-latitude TP, causing more precipitation over the TP.'

"Line 315: It would be very instructive to overlay the 'ktrop' model level on figures 7 and 8. Is WRF using a terrain-following vertical coordinate? I imagine that the 'lid' is not horizontal at all - does that change your conclusions about how and where the nudging is applied?"

Author Response: Thanks for your comments and suggestions. As shown in new Figure 7 and Figure 8, the 'ktrop' model level has been added in the revised manuscript and relevant explanation is available at Line: 308-311.

In this study, the WRF model used "Hybrid Vertical Coordinate". As explained by the WRF source code documentation 'README.hybrid_vert_coord' (https://github.com/NCAR/WRFV3/blob/master/README.hybrid_vert_coord), the hybrid vertical coordinate are terrain following near the surface, but then relax towards an isobaric surface aloft. The purpose of this coordinate option is to reduce the artificial influence of topography towards the top of the model.

Yes, you are correct. This lid is indeed not horizontal. Ideally, the user-defined lid (KTROP) is selected to represent the tropopause, and will be refined or supplemented with the space and time varying tropopause. The variability of the tropopause over the Tibetan Plateau (TP) is complicated during summer. In this study, it is an effective way to select a certain pressure layer in the model vertical layers representing the tropopause as the lid. It does not change our conclusions about how and where the nudging is applied.

"Line 395: If I understand you correctly, the best results were achieved with SNnoT, nudging only the winds and geopotential, from the top of the PBL through the domain top, while not forcing the temperature and humidity at all?"

Author Response: Thank you for this comment. Yes, your understanding are correct. The best results in improving the simulation of the intensity and diurnal cycle of precipitation were achieved when spectral nudging was applied towards winds and geopotential and not forcing the temperature and humidity at all. The reasons can be summarized as follows:
In this study, we have already run the sensitive experiments of nudging toward temperature and humidity on precipitation simulations, such as:
EXP1, 'SN', with nudging towards horizontal wind components (U, V), temperature (T) and geopotential height (G), and their nudging coefficients were all set to 0.0003 s^{-1}.
EXP2, 'SNlowT' with nudging towards U, V, T and G, but the nudging coefficient of T was 0.000045 s^{-1};
EXP3, 'SNnoT' with nudging toward U, V and G only;
EXP3, 'SNQ_trop25' with nudging towards U, V, T, G and Q, while restricting nudging towards T and Q above the model layer of 25 (the lower limit for the 'lid' layer);
EXP4, 'SNQ_trop39' is same as 'SNQ_trop25' but restricting nudging towards T and Q above the model layer of 39 (approximate the tropopause layer).
A new Figure 6 has been given to evaluate above experiments for column-integrated water vapor transport. Compared to ERAI (Figure 6a1) and ERA5 (Figure 6b1), SN (Figure 6d1) misrepresented the large-scale northward water vapor transport. The impact of nudging towards temperature can be found in the comparison between SNlowT (Figure 6f1) and SNnoT (Figure 6g1), in which SNlowT simulated much stronger northward water vapor transport than SNnoT over the southeastern TP. This excessive water vapor transport can also be observed in SNQ_trop25 (Figure 6h1 and Figure 6h2) and SNQ_trop39 (Figure 6i1 and Figure 6i2).
A new Figure 7 has been given to evaluate the impact of nudging on convection over the southern slope of the Himalayas. From the Figure 7g, the strongest upward wind was simulated by SNQ_trop39, followed by SN (Figure 7b) and SNQ_trop25 (Figure 7f). In this case, large amounts of water vapor can be transported to the upper troposphere by strong upward motion, and then conveyed to the interior of the TP through upper-level atmospheric circulation. The upward motion over the southern slope of the Himalayas simulated by the SNnoT (Figure 7e) showed a clear reduction. Therefore, most of the water vapor were condensed in upslope flow over the Himalayas, causing less water vapor available for precipitation over the interior TP.
Accordingly, the smallest RMSE and MAE of precipitation simulation were achieved by SNnoT (Figure 4) rather than SNlowT, SNQ_trop25 or SNQ_trop39. In addition, larger RMSEs and MAEs were obtained when nudging towards humidity was applied. Therefore, spectral nudging was applied towards winds and geopotential only while not forcing the temperature and humidity at all.

Aforementioned new Figure 6 and Figure 7 have been added in the revised manuscript and relevant descriptions have also been added in ‘Section 4.1’ (Line: 278-301) and ‘Section 4.2’ (Line: 312-331), respectively.

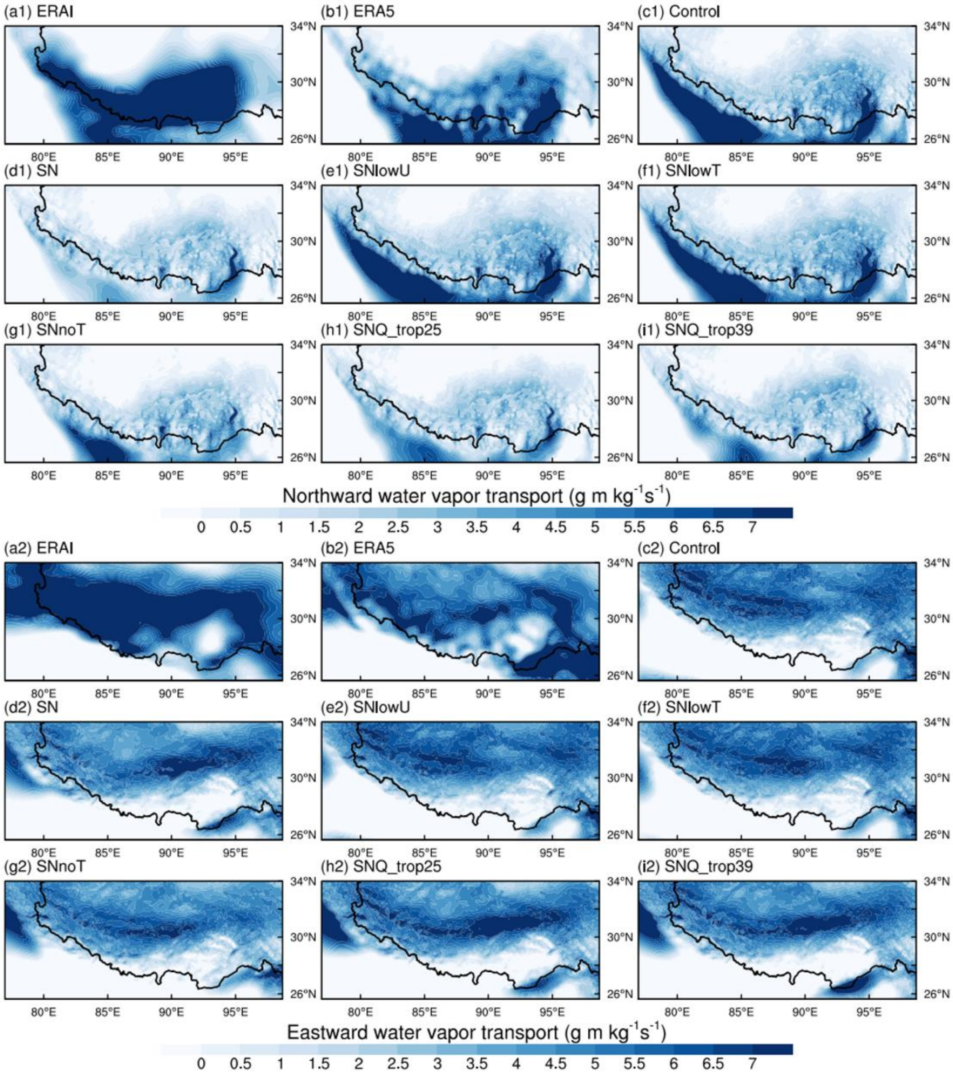

Figure 6: Column-integrated northward water vapor transport (meridional wind component multiples by specific humidity, units: g m kg^{-1} s^{-1}) averaged over the study period over the central Himalayas derived from (a1) ERAI (ERA-Interim), (b1) ERA5, (c1) Control, (d1) SN, (e1) SNlowU, (f1) SNlowT, (g1) SNnoT, (h1) SNQ_trop25 and (i1) SNQ_trop39, respectively. (a2)-(i2) are the same as (a1)-(i1) but for the eastward water vapor transport (zonal wind component multiples by specific humidity).

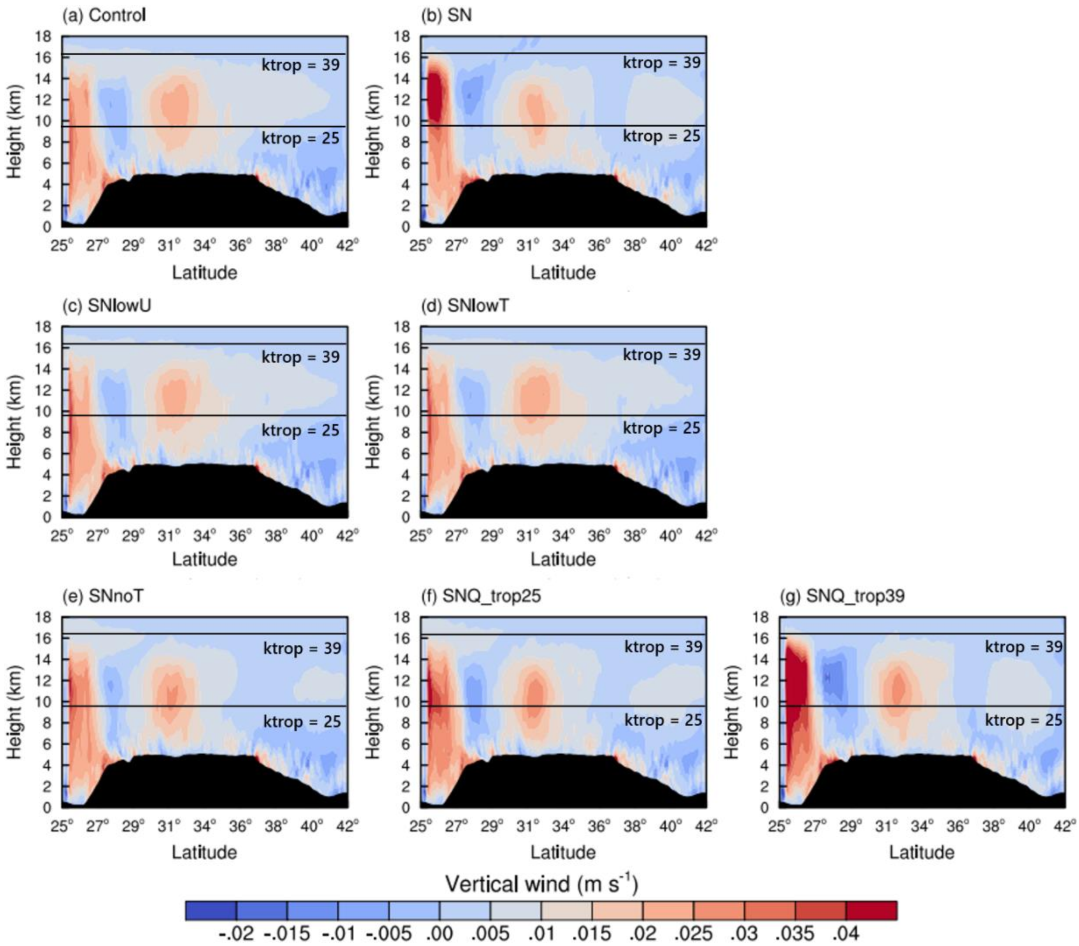

Figure 7: Vertical wind (m s^{-1}; positive value means upward wind and negative value means downward wind) averaged over the study period along the average of 92-102 °E cross section derived from (a) Control, (b) SN, (c) SNlowU, (d) SNlowT, (e) SNnoT, (f) SNQ_trop25 and (g) SNQ_trop39. Black solid lines represent the height of 'ktrop' layer of 25 and 39.

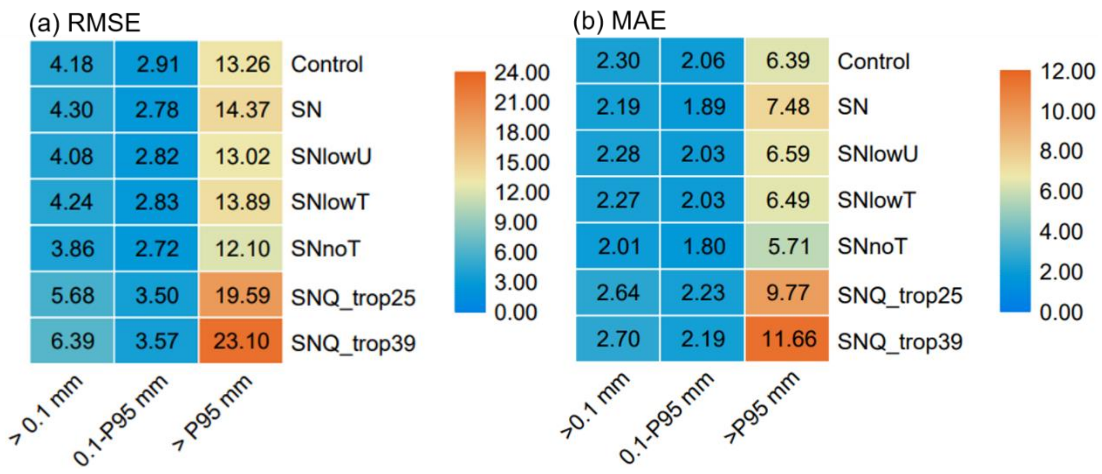

Figure 4: Root mean square error (RMSE) and mean absolute error (MAE) of precipitation (mm day^{-1}) from WRF simulations against CMORPH at different precipitation threshold (P95: monthly mean precipitation intensity at 5.73 mm day^{-1}). Color shading represents the performance of each WRF simulation, where more intense blue indicates a smaller bias of

simulation and more intense orange indicates a larger bias of simulation.

References:
Dong, W. H., Lin, Y. L., Wright, J. S., Ming, Y., Xie, Y. Y., Wang, B., Luo, Y., Huang, W. Y., Huang, J. B., Wang, L., Tian, L. D., Peng, Y. R., and Xu, F. H.: Summer rainfall over the southwestern Tibetan Plateau controlled by deep convection over the Indian subcontinent, Nat Commun, 7, 2016.
Hong, S. Y., Noh, Y., and Dudhia, J.: A new vertical diffusion package with an explicit treatment of entrainment processes, Mon Weather Rev, 134, 2318-2341, Doi 10.1175/Mwr3199.1, 2006.
Juang, H. M. H., and Kanamitsu, M.: The Nmc Nested Regional Spectral Model, Mon Weather Rev, 122, 3-26, 1994.
Kanamaru, H., and Kanamitsu, M.: Scale-selective bias correction in a downscaling of global analysis using a regional model, Mon Weather Rev, 135, 334-350, 2007.
Waldron, K. M., Paegle, J., and Horel, J. D.: Sensitivity of a spectrally filtered and nudged limited-area model to outer model options, Mon Weather Rev, 124, 529-547, 1996.
Wang, Y., Yang, K., Zhou, X., Chen, D. L., Lu, H., Ouyang, L., Chen, Y. Y., Lazhu, and Wang, B. B.: Synergy of orographic drag parameterization and high resolution greatly reduces biases of WRF-simulated precipitation in central Himalaya, Clim Dynam, 54, 1729-1740, 10.1007/s00382-019-05080-w, 2020.